

Electroactive polyimide based on aniline nonamer

Hanfu WANG(王汉夫) Jiatao Zhou(周家涛) Xuepeng QIU*(邱雪鹏)

Polymer Composites Engineering Laboratory, Changchun Institute of Applied Chemistry, Chinese Academic of Sciences, Changchun, 130022, P. R. China

(中国科学院长春应用化学研究所高分子复合材料工程实验室)

* Correspondence to: Xuepeng Qiu E-mail: xp_q@ciac.ac.cn

Abstract Main-chain structured electroactive polyimide based on aniline nonamer was obtained *via* oxidative coupling from monodispersed tetraaniline precursor. The structure of the polyimide as well as its electrochemical properties was studied by UV-*vis* and cyclic voltammetry. Anti-corrosion ability of the polyimide was compared with its pentaaniline analogue. Results show that extending in conjugating length of oligoaniline segments can facilitate intramolecular or intermolecular charge transportations, and increase function efficiency of the materials during practical applications.

Key words: Aniline oligomer, oxidative coupling, conducting polyimide, anti-corrosion

1. INTRODUCTION

Polyimides have been recognized as excellent engineering materials and used in numerous applications ranging from aerospace to microelectronics. [1-3] Ring-like imide structures on polyimide's backbone endow the polymer with extraordinary thermal stability as well as unique mechanical strength, making it a perfect choice for applications under extreme conditions. [4] While, with technology developed, new aspects for polyimide are needed. One of these issues is the electronic conducting property which is quite crucial for technologies of radar wave stealth or electromagnetic interference shielding. [5] To gain a better efficiency, higher electronic conductivity has to be achieved. However, polyimide is actually an electronic insulator. Its volume resistivity is about $10^{16}\Omega \cdot \text{cm}$, which is far away from the standard value (approximately $10^2\Omega \cdot \text{cm}$) for practical applications. [6]

To solve the problem, various efforts have been tried. Traditional methods to raise the conductivity of polyimide is blending with electroactive materials such as metal particles, [7] carbon black, [8] carbon nanotube [9] or graphene. [10] Even conducting polymers [11] have also been introduced into the polyimide matrix. Though the methods have been proven to be functional, serious questions such as macroscopic phase separations or mechanical performance decreases were still left unable to solve.

As an alternative choice, intrinsically conductive polyimide is paid more and more attentions recently. By co-polymerizing electroactive monomers into the polymer backbones, macroscopic phase separations could be suppressed, allowing the material to exhibit certain conductivity while still can maximally maintain its mechanical superiority. Among the various candidates, amine-capped aniline oligomer [12] is no doubt the most proper one suitable for polyimide. Apart from its relative lower cost, aniline oligomers can also offer higher environmental stability and easier processing ability compared with the other candidates.

In 1998, Wang and Wei [13, 14] gave the first report on synthesis and electroactive properties of an oligoaniline-based polyimide. Amine-capped aniline trimer was co-polymerized with 4,4'-oxydianiline (ODA) and 4,4'-(hexafluoroisopropylidene) diphthalic anhydride (6FDA) under refluxing *m*-cresol. The polymer exhibited good solubility in common solvents such as tetrahydrofuran (THF), N, N-dimethylformamide (DMF), dimethyl sulfoxide (DMSO), and NMP, and could be cast into tough thin films. A glass transition temperature was detected to be near 300°C and the onset temperature for 5% weight loss in nitrogen

was above 500 °C. Electrochemical studies revealed that the polymer shows relative higher oxidation resistance compared with its aniline oligomeric analogues. By oxidative coupling of oligoaniline-containing precursor, polyimide that possesses aniline pentamer was also obtained.^[15] The polymer exhibited a similar electrochemical character as polyaniline. While, its electrical conductivity was detected as $8.87 \times 10^{-6} \text{ S} \cdot \text{cm}^{-1}$, still lower than polyaniline.

The problem of low conductivity for the polyimides prepared both *via* polycondensation or oxidative coupling is probably caused by limitations in conjugating length of the oligoaniline segments. To gain a better charge migrating or transporting ability, longer oligoaniline segments are required to provide enough spaces for de-localization of the π -conjugating electrons. In this manuscript, polyimide that contains aniline nonamer was prepared for the first time. By extending the repeating units of oligoaniline segments, some new aspects for the polyimide were discovered.

2. EXPERIMENTAL

Materials

N-Phenyl-*p*-phenylenediamine (98%) (PPDA) was purchased from Aldrich and used without further purification. Iron chloride hexahydrate, Ammonium persulfate (98%) (APS), Phenylhydrazine (98%) were purchased from Shanghai Aladin Reagent Co. Ltd.. 3,3',4,4'-benzophenonetetracarboxylic dianhydride (BTDA) was purchased from Changzhou Sunlight Pharmaceutical Co. Ltd., it was dried under 180°C in an oven before use. Common solvents were purchased from Beijing Chemical Factory.

Synthesis of tetramer precursor (M4AA)

Amine/phenyl-capped aniline tetramer was prepared according to the method reported by Zhang.^[16] PPDA was oxidized simultaneously by iron chloride hexahydrate in 1M HCl aqueous solution under vigorously stirring. After anti-doping with 1.0 M ammonium hydrate aqueous solution, the emeraldine base state (EB state) oligomer was further reduced by phenyl hydrazine in DMF. The white powder collected through recrystallization from ethanol was dried under vacuum and used directly for the following reaction.

3.66 g (10 mmol) LEB amine/phenyl-capped tetraaniline was dissolved in 100 mL NMP. 1.07 g (3.33 mmol) dried BTDA was added into the solution. It was stirred for 24h under N₂ before pouring into deionized water. The solid precipitate collected was washed with ethanol for several times and dried under vacuum.

FTIR (KBr, cm⁻¹): 3403 (m, ν_{NH}), 3025 (m, ν_{CH} of benzenoid rings), 1717 (m, $\nu_{\text{C=O}}$ symmetric stretching), 1601 ((s, $\nu_{\text{C=C}}$ of quinoid rings), 1505 (s, $\nu_{\text{C=C}}$ of benzenoid rings), 1381 (s, $\nu_{\text{C-N}}$), 1298 (s, N=Q=N, where Q represents the quinoid rings), 820 (m, δ_{CH}), 743 (m, imide ring deformation).

¹H NMR (d⁶-DMSO): δ = 8.24 (d, 2H, proton signal on BTDA), 8.14 (m, 4H, proton signal on BTDA), 8.07 (s, 2H, proton signal of -NH- on tetraaniline), 7.80 (s, 2H, proton signal of -NH- on tetraaniline), 7.75 (s, 2H, proton signal of -NH- on tetraaniline), 7.29-6.93 (m, 32H, protons on tetraaniline benzenoid rings), 6.69 (t, 2H, terminal protons on benzenoid rings)

Elemental analysis: C₆₅H₄₆N₈O₅, Calcd. C 76.61, H 4.55, N 11.00, O 7.85; Found C 76.60, H 4.49, N 10.98, O 7.93.

Synthesis of nonaaniline polyimide (A9I)

2.11 g (2.0 mmol) M4AA and 0.22 g (0.2 mmol) *p*-phenylenediamine were dissolved in 50 mL NMP mixture solvent (40 mL NMP, 5 mL deionized water and 5 mL concentrated HCl). 0.91 g APS (4.0 mmol) was dissolved in 10 mL 1.0M HCl and added dropwise into the solution of M4AA at room temperature. The reaction was continuously stirred for 24h before being precipitated from 500 mL deionized water. The solid product obtained was rinsed with THF for several times and dried under vacuum.

FTIR (KBr, cm⁻¹): 3262 (m, ν_{NH}), 1701 (m, $\nu_{\text{C=O}}$ symmetric stretching), 1651 ((s, $\nu_{\text{C=C}}$ of quinoid rings), 1503

(s, $\nu_{C=C}$ of benzenoid rings), 1299 (s, ν_{C-N}), 1129 (s, $N=Q=N$, where Q represents the quinoid rings), 981 (m, δ_{CH}), 805 (m, δ_{CH}).

Reduction of nonaaniline polyimide was realized by stirring with hydrazine hydrate in ammonium hydroxide solution.

Imidization of nonaaniline polyimide was realized by vacuum thermo-imidization under 300°C for 4h.

Characterizations

Fourier-transform infrared

FTIR was recorded on VERTEX70 Spectrometer by averaging 128 scans at a solution of 4 cm^{-1} in the range of 4000–400 cm^{-1} . The samples were mixed with KBr and pressed into a plate for measurement at roomtemperature.

MALDI-TOF-MS

Matrix-Assisted Laser Desorption/ Ionization Time of Flight Mass Spectrometry (MALDI-TOF-MS) was performed on anAXIMA-CFR laser desorption ionization flyingtime spectrometer (COMPACT).

¹H NMR

¹H NMR spectra were run on a BRUKER-400 spectrometer. d⁶-DMSO was used as solvent

Elemental analysis

Wight percentages of carbon, hydrogen and nitrogen of the sample were analyzed by Flash Ea 1112 instrument.

UV-vis

UV-vis spectra for the aniline precursor and polyimide were performed on PERSEE T6 instrument. NMP was used as solvent. To give a time-depended oxidation observation, trace amount of APS was add into the sample cell.

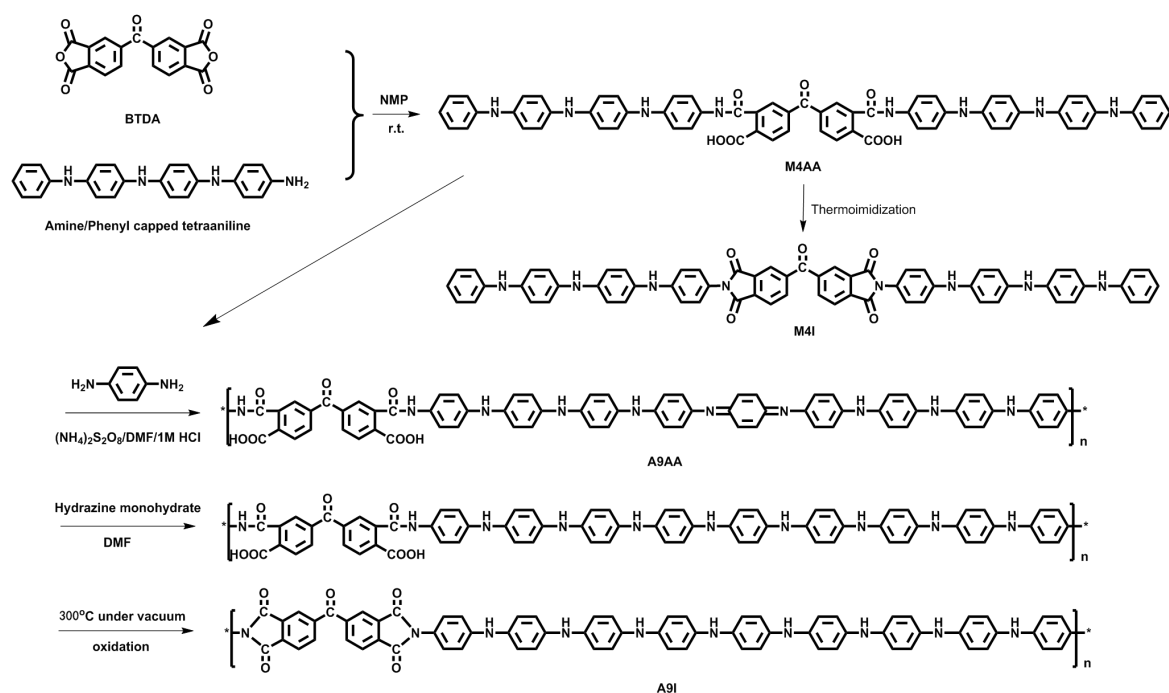
Cyclic voltammetry

The cyclic voltammetry was performed on CHI 660Delectrochemical workstation. 1.0M H₂SO₄ aqueous solution was used as electrolyte. Ag/AgCl electrode was used as reference. NMP solutions of the samples were cast onto glassy carbon electrode and evaporated under infrared lamp. For Tafel curves, iron wire of 1.0 mM diameter was used as working electrode. Samples were dip-coated on the electrode from NMP solutions.

3. RESULTS & DISCUSSION

Synthesis and characterization of nonaaniline polyimide

Synthetic procedure for nonaaniline polyimide is shown in Scheme 1. For convenience, the tetraaniline precursor was named as M4AA. Its imidization form was named as M4I. Correspondingly, the nonaaniline polyamide acid and its imidization form were named as A9AA and A9I respectively.



Scheme 1 Preparation of nonaaniline polyimide

Condensation between BTDA and tetraaniline was conducted in NMP under room temperature. The reaction yielded a light green color powder product on depositing from water. MS spectrum (Figure 1) of M4AA showed two distinguished molecular ionic peaks at 1018 and 1036. The signals were indexed as the structures inserted in the figure. Unexpected imidization of the oligomer was found during detection. The imidization might be caused by overdose laser irradiation, however, it still can be concluded from the spectrum that tetraaniline precursor has been successfully synthesized.

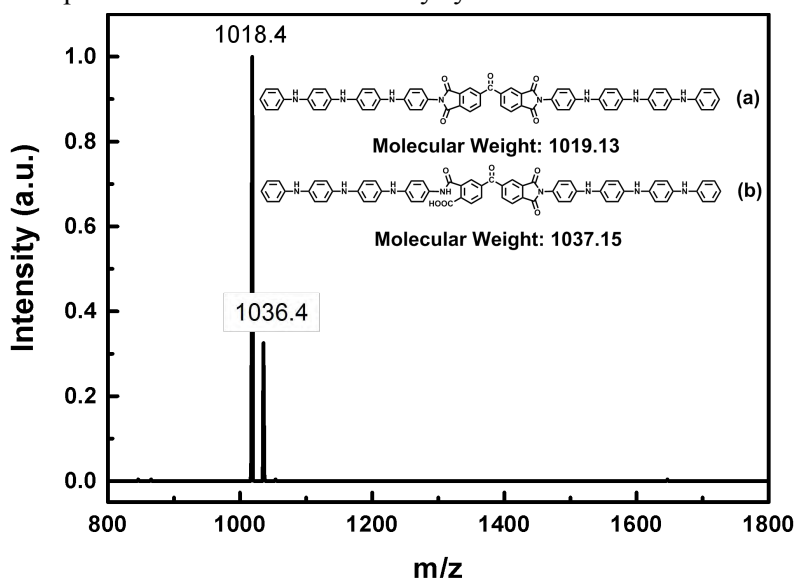


Figure 1 MALDI-TOF-MS of M4AA. Representations in form of formula were shown for signal 1018 and 1036 respectively.

The chemical structure of M4AA can be verified by ¹H NMR as well. Comparison between tetraaniline and M4AA was shown in Figure 2. The amine protons marked as 8 in tetraaniline disappeared in the spectrum of the precursor, suggesting a complete transforming for terminal amines into amides. The signals

for imine protons on nitrogen atoms shifted left-hand into the low-field regions in response to electro-withdraw effects aroused from amide groups. Peak area integrity between protons on benzenoid rings of BTDA is proportional with that of tetraaniline. Therefore, the chemical structure of M4AA is concordant with expectations.

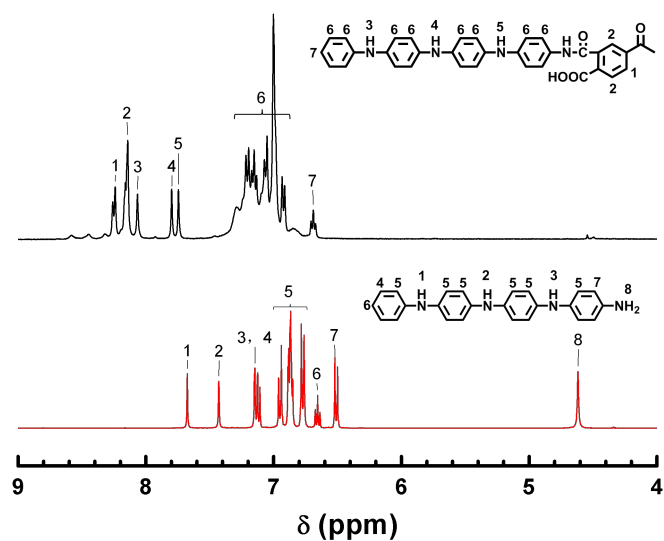


Figure 2 ^1H NMR comparison between tetraaniline (bottom) and M4AA (top). Signal peaks were numbered and indexed as the formula shown above the spectrum.

Oxidation of M4AA by ammonium persulfate yielded a blue black color deposits. Change in color from light-green of M4AA to blue black of A9AA indicates the absorption band of aniline segments shifted to longer wavelength range. During the oxidation process, tetraaniline segments were coupled into nonaaniline segments, giving an extension in conjugating length for the aniline segments. Extension in conjugating length lowers migration barrier for π -conjugating electrons, and decrease π_b - π_q * band gap for the excitons.

^[17]This change can be verified by UV-*vis* comparison between M4I and A9I as was shown in Figure 3.

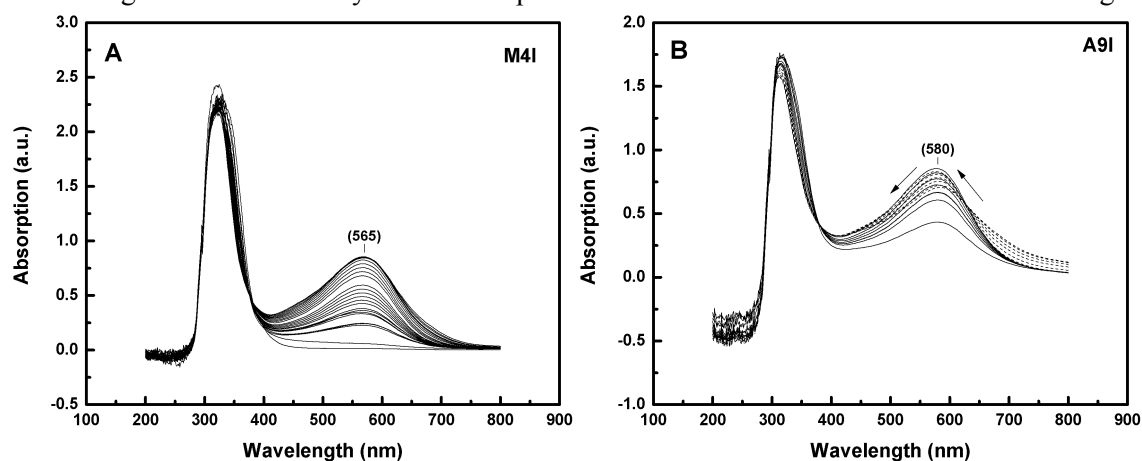


Figure 3 UV-*vis* of M4I (A) and A9I (B). The peak position changing trend was marked with black arrow.

UV-*vis* curves for M4I presented a steady π_b - π_q * absorption band around 565 nm (Figure 3A), whereas, the same band for A9I was found to red shift to 580 nm (Figure 3B). Judging from the comparison, it can be concluded that M4AA has successfully transformed into A9AA.

In addition to the difference of band location, the evolution pattern for the band in response to oxidation was found different for M4I and A9I as well. Unlike M4I, the π_b - π_q * absorption band of A9I

exhibited multiple oxidizing processes. During the process, the peak intensity of the band first went up to a maximal point and then went down gradually. Meanwhile, the peak center showed slightly blue shift after the maximal intensity was achieved. This typical evolution pattern reveals multiple oxidation states for A9I and in turn proves that the oxidative coupling reaction between M4AA has been successfully realized. To make it clear, CV analysis for M4I and A9I were conducted as is shown in Figure 4.

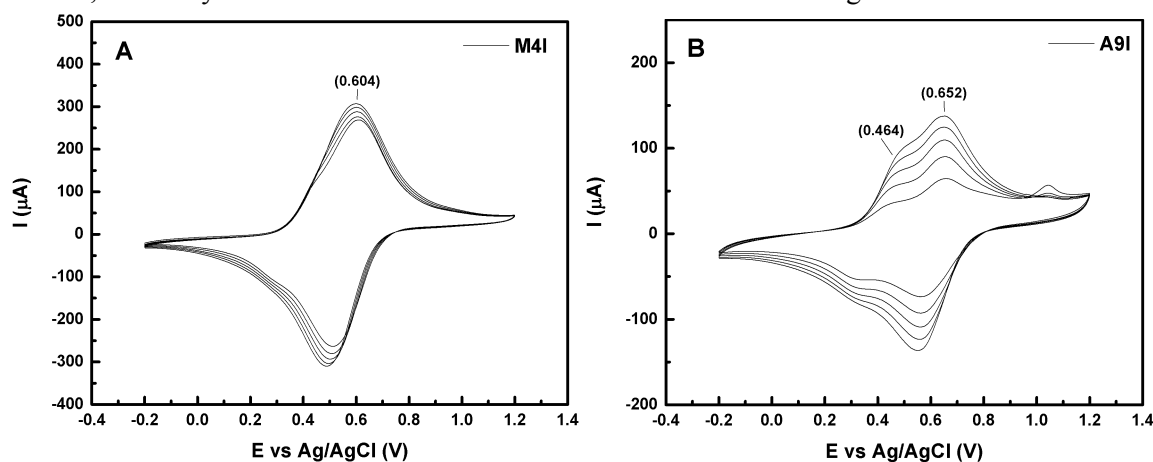


Figure 4 CV curves for M4I (A) and A9I (B). First 10 cycles is recorded with 1.0 M H₂SO₄ aq. solution serving as electrolyte.

For M4I, a strong oxidation peak appears at 0.60V. A tiny shoulder peak was also found around 0.44V which is presumably associated with oxidation of half-side of the precursors. With the scanning repeated, the tiny shoulder peak disappeared gradually. The curves finally stabilized at presence of only one pair of redox peaks. This pair of peaks is corresponding to the transition process shown in Figure 5A. On the other side, the curves for A9I stabilized at presence of two pair of redox peaks which is located at 0.46V and 0.65V respectively. These two oxidation processes are corresponding to the transitions from LEB to EB and EB to PNB respectively (Figure 5B). The difference in oxidation/reduction behavior for M4I and A9I is concordant with the result from UV-*vis*, and therefore, confirmed the structure of nonaaniline polyimide once again.

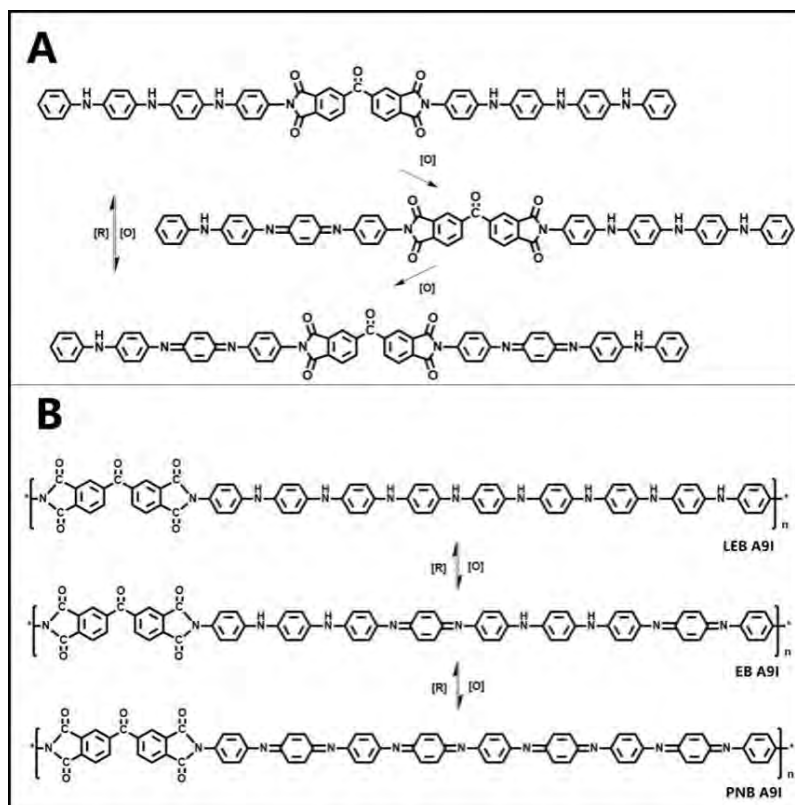


Figure 5 Explanation to oxidation state transitions for M4I (A) and A9I (B)

Anti-corrosion behavior of nonaaniline polyimide

Nonaaniline polyimide possesses nine repeating aniline units between two adjacent BTDA units. Its conjugating length is beyond the limitation of polyimides based on aniline trimer or pentamer. This superiority in length could increase contacting probability between aniline segments and decrease the internal resistance for charge transporting. Decrease in current resistance means better conducting ability. This advance in conductivity may help nonaaniline polyimide to gain a better position during the competition in practical applications.

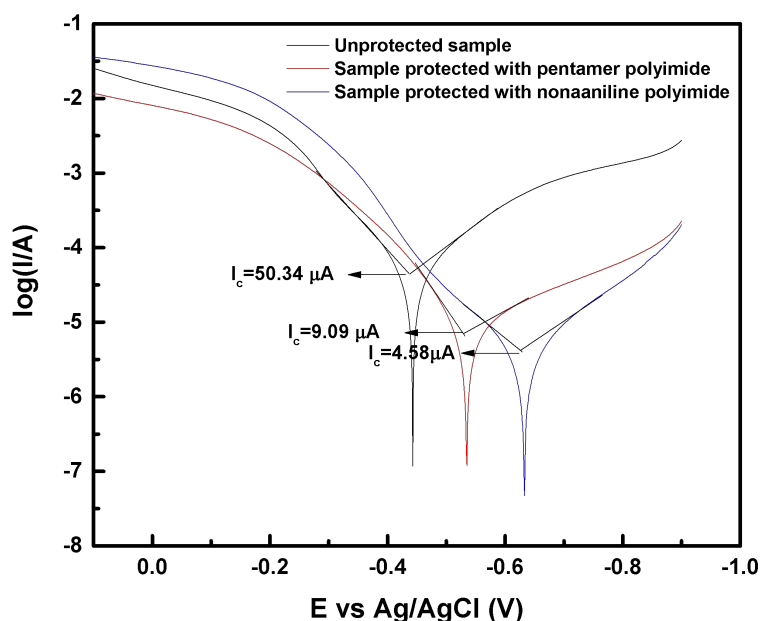


Figure 6 Tafel curves for unprotected (black), pentaaniline polyimide protected (red) and nonaaniline polyimide protected Fe samples. The curves were recorded with 3.5 wt.% NaCl aq. solution.

Figure 6 shows the Tafel curve comparisons between unprotected, pentaaniline polyimide protected and nonaaniline protected Fe samples. The pentaaniline polyimide was synthesized according a similar procedure as nonaaniline polyimide from N-Phenyl-p-phenylenediamine. The corrosion current for these samples is calculated as 50.34, 9.09 and 4.58 μA respectively. Decrease in corrosion current means the corrosion process become more and more difficult because of the protection of the oligoaniline polyimide. Calculated from the curves, nonaaniline polyimide exhibits a protection efficiency of 90%, higher than 78% of pentaaniline polyimide. Considering that all of the parameters were kept same for both of the polymers, it is can be concluded that extension in conjugating length has a positive effect on corrosion resistance of oligoaniline polyimide. This result accords with the original intension of design and widens the application space of oligoaniline based polyimides in the future.

4. CONCLUSION

In all, polyimide based on aniline nonamer was synthesized by oxidative coupling from tetraaniline precursor. Different oxidation structures for polyimide and its tetraaniline precursor were revealed and verified by UV-vis and CV analysis. Nonaaniline polyimide was found to exhibit higher anti-corrosion efficiency compared with its pentaaniline polyimide analogues. Explanation to the increase in protecting efficiency is assumed to be result of charge transportation optimization due to extensions in conjugating length of oligoaniline segments.

Acknowledgement

This work is financially supported by the National Natural Science Foundation of China (20734001, 20904054, and 51173182) and National Key R&D program of China (2017YFB0308300).

References

- [1]. Ding M. X., Polyimides: Chemistry, Relationship between Structure and Properties and Materials, China Science Publishing & Media Ltd., Beijing, 2006.
- [2]. Liaw D. J., Wang K. L., Huang Y. C., Lee K. R., Lai J. Y., Ha C. S., Prog. Polym. Sci.2012, 37, 907-974.
- [3]. Ding M. X., Prog. Polym. Sci.2007, 32, 623-668.
- [4]. Wan M. X., Polym. Bull.1999, 47-53.
- [5]. Liang Z. C., Journal of Instrument Materials 1980, 11, 45-57.
- [6]. Nguyen T. H. L., Cortes L. Q., Lonjon A., *Journal of Non-Crystalline Solid*2014, 385, 34-39.
- [7]. Zhai B. Q., *Physics Experimentation*2010, 30, 15-18.
- [8]. Zhang M., Zhang X., Liu C., Wu Q., Cui Y., *Journal of Functional Materials*2014, 45, 22017-22020.
- [9]. Yoonessi M., Shi Y., Scheiman D. A., Lebron-Colon M., Tigelaar D. M., Weiss R. A., Meador M. A., *ACS Nano*2012, 6, 7644-7655.
- [10]. Han M. G., Im S. S., J. Appl. Polym. Sci.1998, 67, 1863-1870.
- [11]. MacDiarmid A. G., Zhou Y., Feng J., Synth. Met.1999, 100, 131-140.
- [12]. Wang Z. Y., Yang C., Gao J. P., Lin J., Meng X. S., Wei Y., Li S., *Macromolecules*1998, 31, 2702-2704.
- [13]. Lu W., Meng X. S., Wang Z. Y., J. Polym. Sci. Pol. Chem.1999, 37, 4295-4301.
- [14]. Chao D. M., Cui L. L., Lu X. F., Mao H., Zhang W. J., Wei Y., *Eur. Polym. J.*2007, 43, 2641-2647.
- [15]. Zhade Abajo J., de la Campa J. G., *Progress in Polyimide Chemistry I*, Springer-Verlag Berlin: Berlin, 1999.
- [16]. ng W. J., Feng J., MacDiarmid A. G., Epstein A. J., Synth. Met. 1997, 84, 119-120.
- [17]. Honzl J., MetalováM., *Tetrahedron*1969, 25, 3641-3652.